

# **Single-Event Effects Test Report of the TPS50601A-SP Synchronous Step-Down Converter**

## ABSTRACT

The effect of heavy-ion irradiation on the single-event effect performance of the TPS50601A-SP point-of-load switching regulator is presented in this report. Heavy-ions with  $LET_{EFF}$  ranging from 10 to  $\sim 75$  MeV-cm<sup>2</sup>/mg were used to irradiate 7 production devices in 23 experiments with fluences ranging from  $10^7$  to  $10^8$  ions/cm<sup>2</sup> per run. The results show that the TPS50601A-SP is SEL-, SEB-, and SEGR-free across the full electrical specifications and up to  $\sim 75$  MeV-cm<sup>2</sup>/mg. Results also show that the device is SET-free for upsets with deviations higher than  $\pm 5\%$  from the nominal voltage at  $P_{VIN} = V_{IN} = 5$  V,  $V_{OUT} = 2.5$  V,  $L = 4.7$   $\mu$ H,  $C_{OUT} = 660$   $\mu$ F, and up to  $\sim 75$  MeV-cm<sup>2</sup>/mg. Histograms describing all observed upsets inside the  $\pm 5\%$  envelope and worst case time domain plots are presented and discussed.

## Contents

1	Overview .....	3
2	Single-Event Effects .....	4
3	Test Device and Evaluation Board Information .....	5
4	Irradiation Facility and Setup .....	7
5	Depth, Range, and $LET_{EFF}$ Calculation .....	9
6	Test Setup and Procedures .....	10
7	Single-Event-Burnout (SEB), Single-Event-Gate-Rupture (SEGR), and Single Event Latch-Up (SEL) Results .....	13
8	Single-Event-Transient (SET) Results .....	15
9	Event Rate Calculations .....	20
10	Summary .....	21
Appendix A	Total Ionizing Dose From SEE Experiments .....	22
Appendix B	Confidence Interval Calculations .....	23
Appendix C	Orbital Environment Estimations .....	25
Appendix D	References .....	27

## List of Figures

1	Photograph of Delidded TPS50601A-SP [Left] and a Pin-Out Diagram [Right] .....	5
2	TPS50601ASPEVM Board Top-View .....	5
3	Schematic of the TPS50601ASPEVM Used During SEE Testing .....	6
4	Photograph of the TPS50601A-SP Evaluation Board Mounted in Front of the Heavy-Ion Beam Exit Port at the Texas A&M Cyclotron .....	8
5	Generalized Cross Section of the LBC7 Technology BEOL Stack on the TPS50601A-SP [Left] and GUI of RADsim Application Used to Determine Key Ion Parameters [Right] .....	9
6	Block Diagram of SEE Test Setup With the TPS50601A-SP .....	11
7	Current vs Time for SEB Run #6 at Room Temp, 73.28 MeV-cm <sup>2</sup> /mg, 6-A Load, and $P_{VIN} = V_{IN} = 7$ V .....	14
8	Histogram of the Normalized Maximum Value for All Captured SETs Across All $LET_{EFF}$ .....	16
9	Histogram of the Normalized Minimum Value for All Captured SETs Across All $LET_{EFF}$ .....	17
10	Histogram of the Transient Recovery Time for All Captured SETs Across All $LET_{EFF}$ .....	18
11	Time Domain Plot for the Worst Case Positive Deviation Observed .....	18
12	Time Domain Plot for the Worst Case Negative Deviation Observed .....	19
13	Time Domain Plot for the Worst Case Transient Recovery Time Observed .....	19

14	Integral Particle Flux vs $LET_{EFF}$ .....	25
15	Device Cross Section vs $LET_{EFF}$ .....	26

### List of Tables

1	Overview Information .....	3
2	Praseodymium Ion $LET_{EFF}$ , Depth, and Range in Silicon .....	9
3	Equipment Set and Parameters Used for SEE Testing the TPS50601A-SP .....	10
4	Summary of TPS50601A-SP SEB Results .....	13
5	Summary of TPS50601A-SP SEL Results With $T = 125^{\circ}C$ .....	14
6	Summary of TPS50601A-SP SET Results .....	16
7	SEB Event Rate Calculations for Worst-Week LEO and GEO Orbits .....	20
8	SEL Event Rate Calculations for Worst-Week LEO and GEO Orbits .....	20
9	$V_{OUT}$ SET > $\pm 5\%$ From Nominal Voltage and $P_{GOOD}$ Event Rate Calculations for Worst-Week LEO and GEO Orbits .....	20
10	Experimental Example Calculation of Mean-Fluence-to-Failure (MFTF) and $\sigma$ Using a 95% Confidence Interval .....	24

### Trademarks

DuPont, Kevlar are registered trademarks of E.I. du Pont de Nemours and Company.  
 LabVIEW is a trademark of National Instruments Corporation.  
 All other trademarks are the property of their respective owners.

## 1 Overview

The TPS50601A-SP is a space-grade, radiation hardened, 7-V, 6-A synchronous buck point-of-load (POL) converter, which has been optimized for small designs with its high-efficiency operation and integration of the high-side and low-side power MOSFETs into a compact monolithic solution. Further space saving can be achieved through the use of the configurable switching frequency (0.1 to 1 MHz), which can reduce the output filter lumped components. The device is offered in a thermally enhanced 20-pin ceramic, dual in-line flat-pack package. General device information and test conditions are listed in [Table 1](#). For more detailed technical specifications, user-guides, and application notes please go to: [www.ti.com/product/TPS50601A-SP](http://www.ti.com/product/TPS50601A-SP).

**Table 1. Overview Information<sup>(1)</sup>**

TI Part Number	TPS50601A-SP
SMD Number	5962R1022102VSC
Device Function	Point-of-load (POL) Switching Regulator
Technology	250-nm Linear BiCMOS
Exposure Facility	Radiation Effects Facility, Cyclotron Institute, Texas A&M University and Lawrence Berkeley 88-inch cyclotron
Heavy-Ion Fluence per Run	$1 \times 10^7$ to $1 \times 10^8$ ions/cm <sup>2</sup>
Irradiation Temperature	25°C and 125°C (for SEL testing)

<sup>(1)</sup> TI may provide technical, applications or design advice, quality characterization, and reliability data or service providing these items shall not expand or otherwise affect TI's warranties as set forth in the Texas Instruments Incorporated Standard Terms and Conditions of Sale for Semiconductor Products and no obligation or liability shall arise from Semiconductor Products and no obligation or liability shall arise from TI's provision of such items.

## 2 Single-Event Effects

The primary concerns for the TPS50601A-SP are its resilience against the destructive single event effects (DSEE): single event burn-out (SEB), single event gate-rupture (SEGR) and single-event latch-up (SEL). The collected data show that the TPS50601A-SP is SEB-/SEGR-free across the full electrical specifications and up to 75 MeV-cm<sup>2</sup>/mg. Data was collected at room temperature without any temperature force mechanism, a load of 6 A,  $P_{VIN} = V_{IN} = 7$  V, and  $V_{OUT} = 2.5$  V. Under these conditions the die temperature, when mounted on the TPS50601ASPEVM, is around 45°C. The SEB testing was performed at room temperature since it has been shown that SEB susceptibility decrease with incrementing temperature [1] [2].

The TPS50601A-SP was also characterized for SEL events. In mixed technologies such as the Linear BiCMOS process used for the TPS50601A-SP, the presence of CMOS circuitry introduces a potential SEL susceptibility. SEL can occur if excess current injection caused by the passage of an energetic ion is high enough to trigger the formation of a parasitic cross-coupled PNP and NPN bipolar structure (formed between the p-substrate and n-well n+ and p+ contacts) [3] [4]. If formed, the parasitic bipolar structure creates a high-conductance path (creating a steady-state current that is orders-of-magnitude higher than the normal operating current) between power and ground that persists (is “latched”) until power is removed or until the device is destroyed by the high-current state. For the design of the TPS50601A-SP, SEL-susceptibility was reduced by maximizing anode-cathode spacing (tap spacing) while increasing the number of well and substrate ties in the CMOS portions of the layout to minimize well and substrate resistance effects. Additionally, junction isolation techniques were used with buried wells and guard ring structures isolating the CMOS p- and n-wells [5] [6] [7]. The design techniques applied for SEL-mitigation were sufficient as the TPS50601A-SP exhibited absolutely no SEL with heavy-ions of up to  $LET_{EFF} = 75$  MeV-cm<sup>2</sup>/mg at fluences in excess of 10<sup>7</sup> ions/cm<sup>2</sup> and a die temperature of 125°C.

The TPS50601A-SP was characterized for single events transients (SET) using a window trigger of ±5% around the nominal output voltage (~2.5 V ± 125 mV). The device was tested under the following conditions:  $P_{VIN} = V_{IN} = 5$  V,  $V_{OUT} = 2.5$  V, RT = GND, L = 4.7 μH, and  $C_{OUT} = 660$  μF. The output voltage was monitored with a low inductance probe to minimize noise. Also, data was post processed to eliminate data acquisition induced noise, which is not inherent to the TPS50601A-SP. Under this condition, the devices never showed a single upset exceeding the ±5% limits, critical to power up the FPGA, MCU, and CPUs.

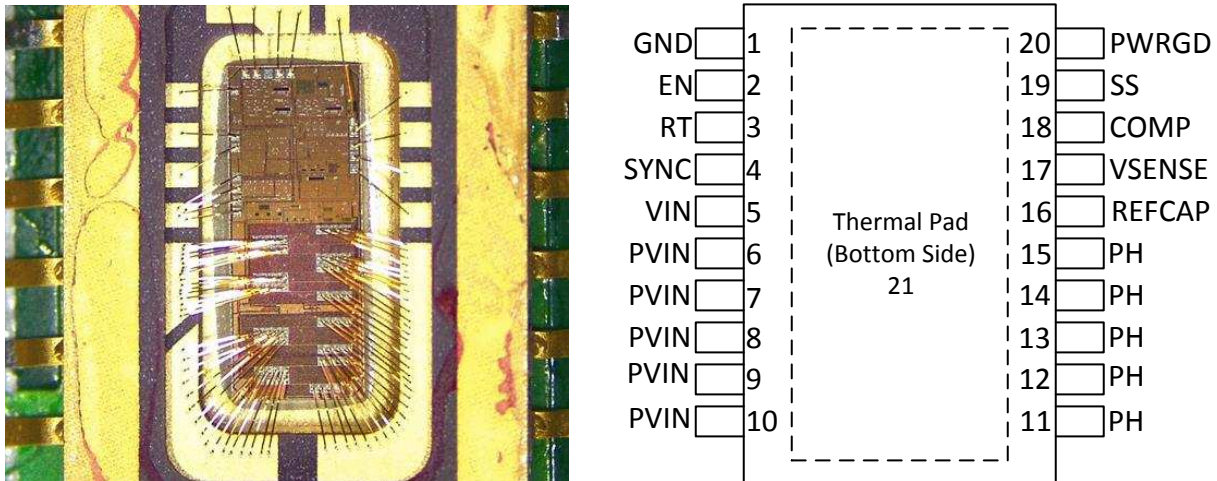
A combination of several different techniques to suppress SET and SEFI were used in the design of the TPS50601A-SP POL. Among these mitigation techniques were the use of triple redundant logic circuits [8], time constant adjustment [9], a new architectural circuit design, and special isolation techniques to prevent latch-up induced by heavy-ions. The efficacy of these techniques was verified by using a custom heavy-ion charge injection model in SPICE, developed specifically for this junction isolated BiCMOS technology. This model was initially developed on theoretical calculations by taking into account specific parameters from the process technology like depletion region depths for different components and doping profiles. The model was then modified based on real heavy-ion measurements. Once adjusted, this model was used to design the different circuit blocks within the TPS50601A-SP POL. The initial model used in SPICE was implemented as a double-exponential function, but it was simplified to a piecewise-linear function to accelerate simulation time [10] [11].

Triple-redundant logic with majority voting was used in critical high-speed logic circuit blocks within the TPS50601A-SP. This reduced the probability of SEFI in sensitive logic. Time-constant adjustment was implemented in digital logic that is not speed-sensitive and in analog circuit blocks. This design technique consisted of reducing on-state series resistance ( $R_{DSon}$ ) of sensitive transistors, increasing storage capacitance in sensitive nodes, and increasing biasing currents in analog functions like the band-gap reference and error amplifier. These techniques were successful since the TPS50601A-SP did not exhibit any SEFI behavior.

### 3 Test Device and Evaluation Board Information

The TPS50601A-SP is packaged in a 20-pin thermally-enhanced dual ceramic flat pack package (HKH) as shown in Figure 1. The TPS50601ASPEVM-S evaluation board was used to evaluate the performance and characteristics of the TPS50601A-SP under heavy-ions. Top view of the evaluation board used for radiation testing is shown in Figure 1. Board schematics are presented in Figure 3. For more information about the evaluation board please go to:

[www.ti.com/tool/tps50601aspevm-s](http://www.ti.com/tool/tps50601aspevm-s)



NOTE: The package lid was removed to reveal the die face for all heavy-ion testing.

**Figure 1. Photograph of Delidded TPS50601A-SP [Left] and a Pin-Out Diagram [Right]**



**Figure 2. TPS50601ASPEVM Board Top-View**

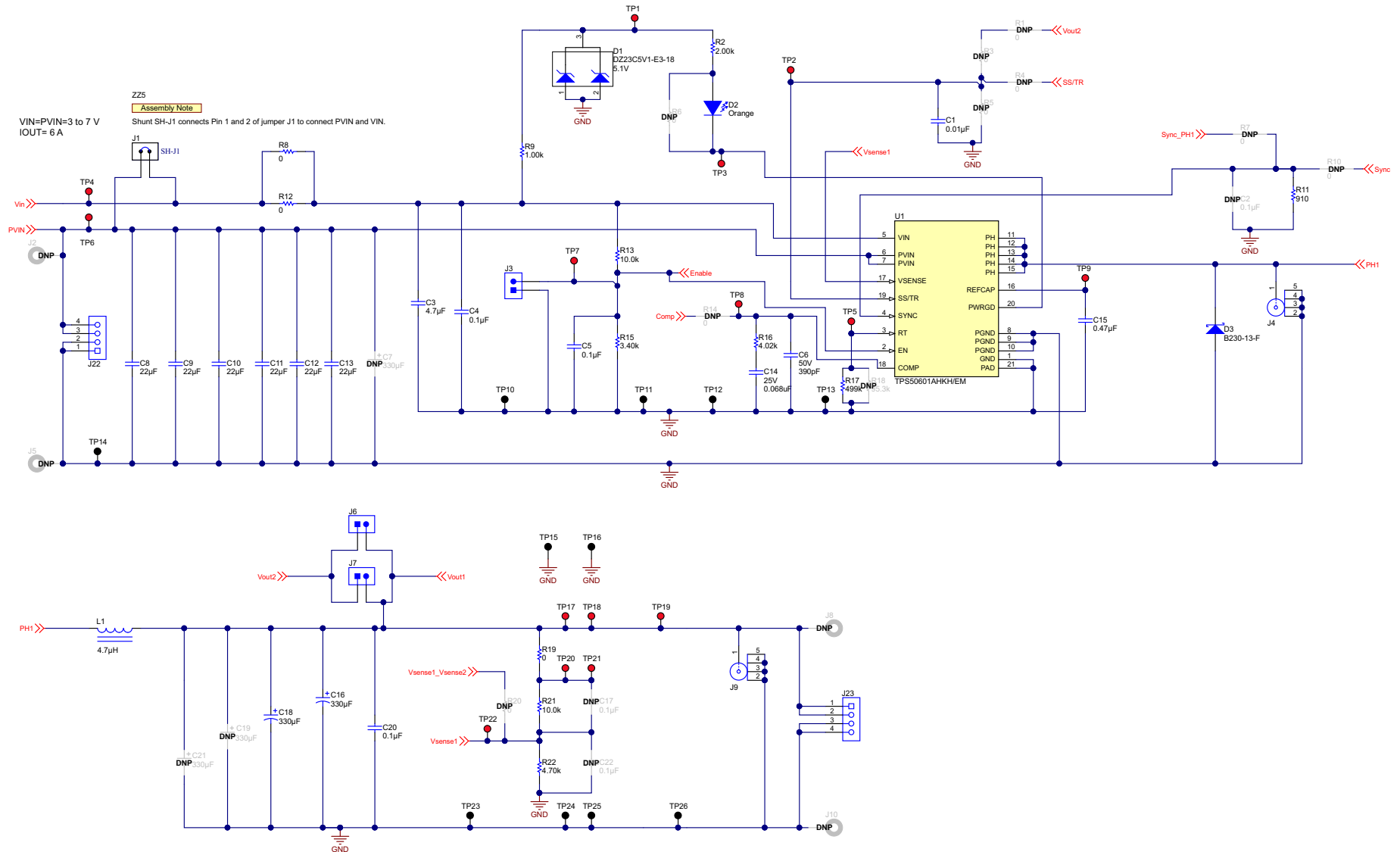


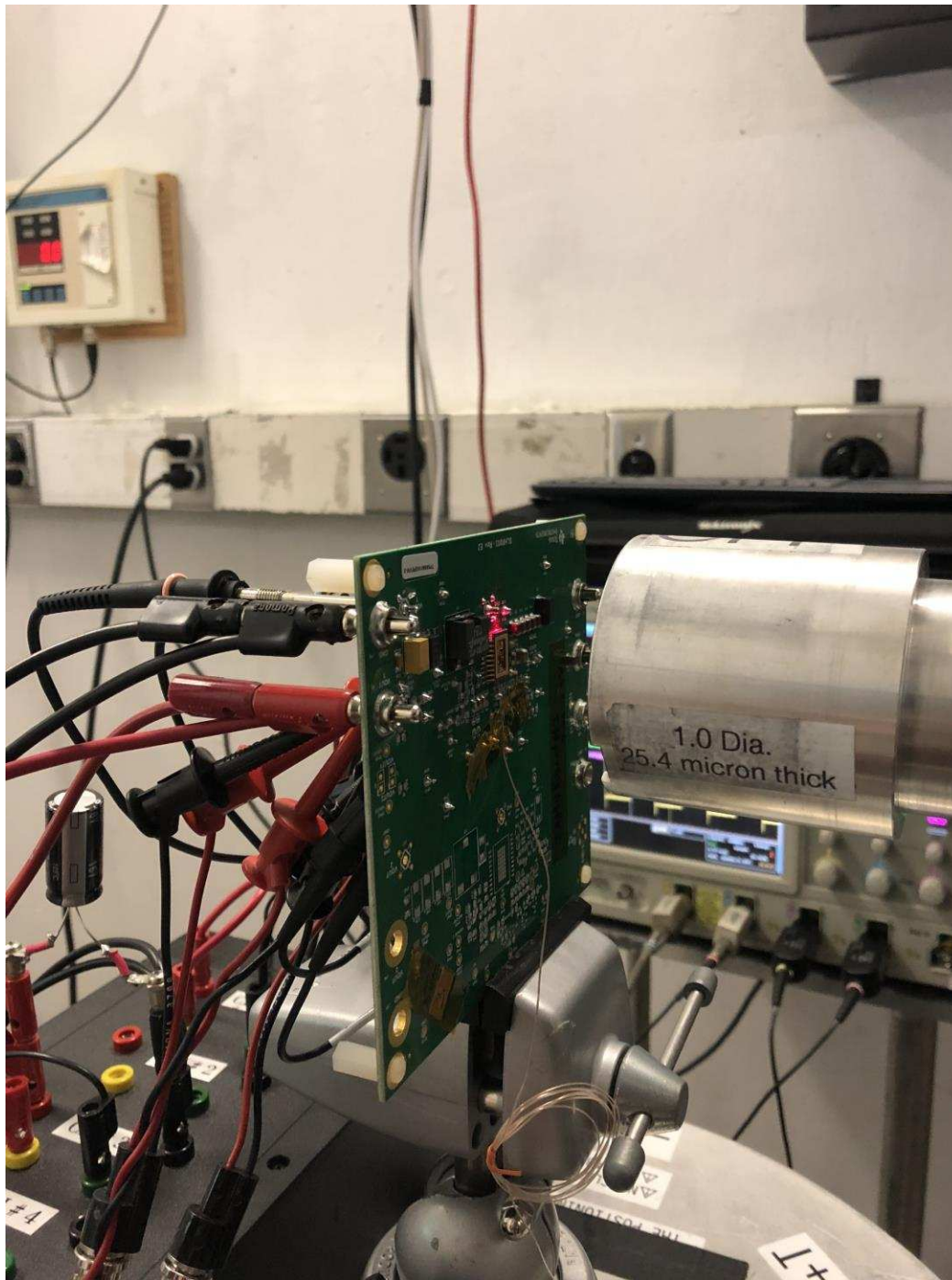
Figure 3. Schematic of the TPS50601ASPEVM Used During SEE Testing

## 4 Irradiation Facility and Setup

The heavy-ion species used for the SEE studies on this product were provided and delivered by the TAMU Cyclotron Radiation Effects Facility [12], and the Lawrence Berkeley 88-inch cyclotron, using a superconducting cyclotron and advanced electron cyclotron resonance (ECR) ion source. At the fluxes used, ion beams had good flux stability and high irradiation uniformity over a 1-in diameter circular cross sectional area for the in-air station (TAMU) and vacuum chamber (Berkeley). Uniformity is achieved by means of magnetic defocusing. The flux of the beam is regulated over a broad range spanning several orders of magnitude. For the bulk of these studies, ion fluxes between  $4.3 \times 10^4$  and  $1.45 \times 10^5$  ions/s-cm<sup>2</sup> were used to provide heavy-ion fluences between  $4.19 \times 10^6$  and  $10^8$  ions/cm<sup>2</sup>.

For these experiments, Argon (<sup>40</sup>Ar), Copper (<sup>63</sup>Cu), Silver (<sup>109</sup>Ag), Xenon (<sup>136</sup>Xe), and Praseodymium (<sup>141</sup>Pr) at angles of 0° and 28° ions were used for LET<sub>EFF</sub> of 10.11 to ~75 MeV-cm<sup>2</sup>/mg. The ions used had a total kinetic energy of 400 MeV to 2.114 GeV, in the vacuum (15-MeV/amu line at TAMU and 10-MeV/amu at Berkeley).

The TPS50601A-SP test board used for the experiments at the TAMU facility is shown in [Figure 4](#). Although not visible in this photo, the beam port has a 1-mil Aramica (DuPont® Kevlar®) 1-in diameter window to allow in-air testing while maintaining the vacuum within the accelerator with only minor ion energy loss. The air space between the device and the ion beam port window was maintained at 40 mm for all runs in TAMU. Lawrence Berkeley 88-inch cyclotron did not provide an in-air solution and rather the device is tested in a vacuum chamber.



NOTE: Probes are connected on the back side.

**Figure 4. Photograph of the TPS50601A-SP Evaluation Board Mounted in Front of the Heavy-Ion Beam Exit Port at the Texas A&M Cyclotron**

### 5 Depth, Range, and LET<sub>EFF</sub> Calculation

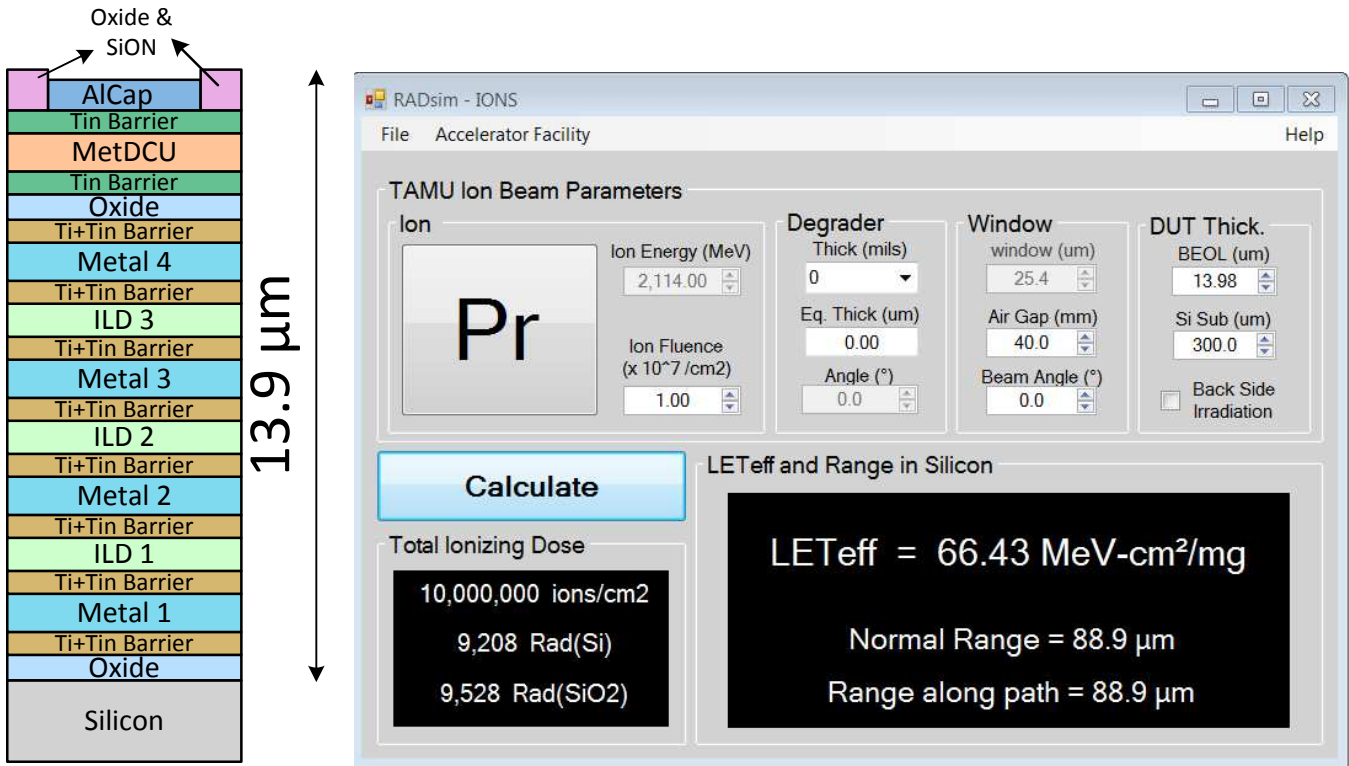


Figure 5. Generalized Cross Section of the LBC7 Technology BEOL Stack on the TPS50601A-SP [Left] and GUI of RADsim Application Used to Determine Key Ion Parameters [Right]

The TPS50601A-SP is fabricated in the TI Linear BiCMOS 250-nm process with a back-end-of-line (BEOL) stack consisting of four levels of standard thickness aluminum metal on a 0.6-μm pitch and damascene copper (Cu). The total stack height from the surface of the passivation to the silicon surface is 13.9 μm based on nominal layer thickness as shown in Figure 5. No polyimide or other coating was present; the uppermost layer was the nitride passivation layer (PON). Accounting for energy loss through the 1-mil thick Aramica beam port window, the 40-mm air gap (valid for TAMU), and the BEOL stack over the TPS50601A-SP, the effective LET (LET<sub>EFF</sub>) at the surface of the silicon substrate, the depth, and the ion range was determined with the custom RADsim - IONS application (developed at Texas Instruments and based on the latest SRIM-2013 [13] models). The results are shown in Table 2. The stack was modeled as a homogeneous layer of silicon dioxide (valid since SiO<sub>2</sub> and aluminum density is similar).

Table 2. Praseodymium Ion LET<sub>EFF</sub>, Depth, and Range in Silicon

ION TYPE	ANGLE OF INCIDENCE (°)	DEPTH IN SILICON (μm)	RANGE IN SILICON (μm)	LET <sub>EFF</sub> (MeV-cm <sup>2</sup> /mg)	Facility
Ar	0	115.8	115.8	10.26	Berkeley
Cu	0	94.6	94.6	22.13	Berkeley
Ag	0	75.7	75.7	51.31	Berkeley
Xe	0	74.4	74.4	63	Berkeley
Xe	28	64.1	72.6	71.78	Berkeley
Pr	0	88.9	88.9	66.43	Texas A&M
Pr	28	77.7	87.2	74.82	Texas A&M

## 6 Test Setup and Procedures

SEE testing was performed on a TPS50601A-SP device mounted on a TPS50601ASPEVM-S, 6-A, Regulator Evaluation Module. Power was provided to the device by means of the PVIN input on the J2 and J5 banana connectors using the N6702 precision power supply in a 4-wire configuration. The PVIN and VIN were tied together using the J1 jumper on the EVM. The device was loaded using a discrete power resistor dissipating 6 A.

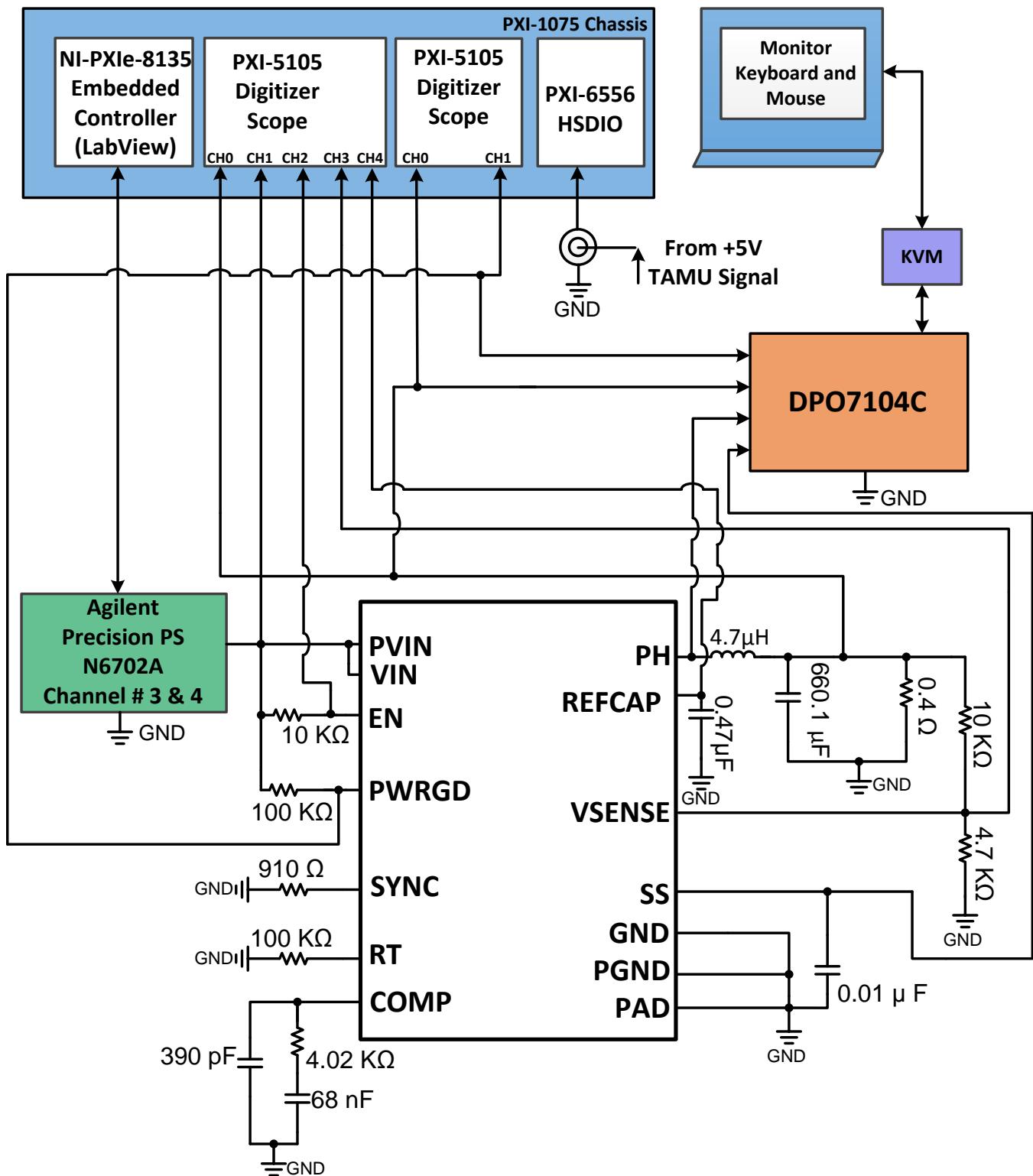
The SEE events were monitored using two National Instruments (NI) PXIe 5105 (60 MS/s and 60 MHz of bandwidth) digitizer modules and one Tektronix DPO7104C Digital Phosphor Oscilloscope (DPO) with 4 channels, 40 GS/s and 2.5 GHz of bandwidth. The DPO was used to monitor the Soft Start (SS), Phase (PH),  $V_{OUT}$ , and  $P_{GOOD}$  signals and was triggered from the SS using a negative edge trigger of 0.5 V. No soft-start upset was observed during any of the runs. The trigger was set to 0.5 V because this is the voltage that will induce a soft-start cycle on the internal logic.

The first NI-PXIe Scope card (#1) was used to monitor  $V_{OUT}$ ,  $V_{IN}$ ,  $P_{GOOD}$ ,  $V_{SENSE}$ , EN, and REFCAP and was triggered from  $V_{OUT}$  using a window trigger set as low as 3% from the nominal output voltage. The second NI-PXIe Scope card (#2) was used to monitor  $P_{GOOD}$  and  $V_{OUT}$  and was triggered from  $P_{GOOD}$  using an edge negative trigger at 2.5 V. With the exception of the DPO digital oscilloscope, all equipment was controlled and monitored using a custom-developed LabVIEW™ program (PXI-RadTest) running on a NI-PXIe-8135 Controller. A block diagram of the setup used for SEE testing the TPS50601A-SP is illustrated in [Figure 6](#) and the connections, limits and compliance used are shown in [Table 3](#). In general, the TPS50601A-SP was tested at room temperature (no external heating applied) where the die temperature was usually  $\approx 40^{\circ}\text{C}$  to  $45^{\circ}\text{C}$  under maximum load conditions. A die temperature of  $125^{\circ}\text{C}$  was used for SEL testing and was achieved with a convection heat gun aimed at the die. The die temperature was monitored during the testing using a K-Type thermocouple attached to the heat slug of the package with solder paste.

**Table 3. Equipment Set and Parameters Used for SEE Testing the TPS50601A-SP**

PIN NAME	EQUIPMENT USED	CAPABILITY	COMPLIANCE	RANGE OF VALUES USED
PVIN/VIN	Agilent N6702A (Ch #3 and 4)	10 A	10 A	5 V and 7 V
Oscilloscope card	HSDIO NI-PXIe 5105	60 MS/s	—	20 MS/s
Digital Oscilloscope	Tektronix DPO7104C	40 GS/s	—	200 MS/s
Digital I/O	NI PXIe 6556	200 MHz	—	50 MHz

All boards used for SEE testing were fully checked for functionality and dry runs performed to ensure that the test system was stable under all bias and load conditions prior to being taken to the TAMU facility. During the heavy-ion testing, the LabView control program powered up the TPS50601A-SP device and set the external sourcing and monitoring functions of the external equipment. After functionality and stability had been confirmed, the beam shutter was opened to expose the device to the heavy-ion beam. The shutter remained open until the target fluence was achieved (determined by external detectors and counters).



- (1) TPS50601A-SP was mounted on a TPS50601ASPEVM-D, 6-A/12-A, Regulator Evaluation Module.
- (2) The Agilent N6702A provided the precision power input for PVIN and a power suitably-sized resistors was used for the 6-A load.

**Figure 6. Block Diagram of SEE Test Setup With the TPS50601A-SP**

During irradiation the PXIe-5101 scope card continuously monitored the Soft Start, Phase,  $V_{OUT}$  and  $P_{GOOD}$  outputs of the TPS50601A-SP. With any deviation going low or high on  $V_{OUT}$  (exceeding the window trigger set around the nominal voltage), going low on  $P_{GOOD}$  (edge-negative trigger) at half the input voltage (since this signal is pulled up to  $V_{IN} 5 V / 2 = 2.5 V$ ), and going low (edge-negative trigger) on SS at 0.5 V triggers a capture.

During a trigger event, the digital scope card would capture 30k to 100k samples (the card was continuously digitizing so when triggered, a predefined 20% of the samples that preceded the event were stored). The NI scope cards captured events lasting up to 5 ms (100k samples at 20 MS/s). In parallel, the DPO monitored Soft Start, Phase,  $V_{OUT}$ , and  $P_{GOOD}$  and triggered from Soft Start using a negative edge at 0.5 V. The sample rate was set to 200 MS/s with 5  $\mu$ s/div recording 20% (or 10  $\mu$ s) before the event. The DPO was set to fast frame during the test. Under this configuration, the scope had a 3.2- $\mu$ s update time. The update rate represents the amount of time to re-arm the scope trigger after an event. During the characterization, not a single Soft-Start (SS) trigger (restart cycle) was observed.

In addition to monitoring the voltage levels of the two scopes cards (PXI) and one DPO, the current on the  $P_{VIN}$  and  $V_{IN}$  (tied-together for all test) pins was also monitored during each test to enable separation of SEFI induced state changes from those caused by the occurrence of an SEL event. Outside of normal fluctuations, no sudden increases in current were observed on any of the test runs, indicating that no SEL events occurred.

## 7 Single-Event-Burnout (SEB), Single-Event-Gate-Rupture (SEGR), and Single Event Latch-Up (SEL) Results

### 7.1 Single-Event-Burnout (SEB) and Single-Event-Gate-Rupture (SEGR) Results

SEB and SEGR data was collected at room temperature (no external temperature force element used), full load (6 A) and  $P_{VIN} = V_{IN} = 7\text{ V}$  (maximum operating voltage), and  $V_{OUT} = 2.5\text{ V}$  at  $LET_{EFF}$  of 66.42 MeV-cm<sup>2</sup>/mg and 73.2 MeV-cm<sup>2</sup>/mg. Also data was collected at nominal  $P_{VIN} = V_{IN} = 5\text{ V}$ , 3 A, and 74.8 MeV-cm<sup>2</sup>/mg. As discussed in [Section 2](#), SEB susceptibility decrement with incremented temperature, making it worst case at lower temperatures. For that reason testing was conducted at room temperature.

Under these conditions, the die temperature is around ≈40°C to 45°C (when mounted on the TPS50601ASPEVM). The device was exposed to Praseodymium (<sup>141</sup>Pr) heavy-ions with an angle of incidence of 0° and 28° (at the Texas A&M cyclotron) for an  $LET_{EFF}$  of 66.42 and 74.82 MeV-cm<sup>2</sup>/mg, respectively. Also it was exposed to Xenon (<sup>136</sup>Xe) heavy-ions with an angle of incidence of 30° for an  $LET_{EFF}$  of 73.28 MeV-cm<sup>2</sup>/mg, at the Berkeley 88-inch cyclotron.

Flux of 10<sup>5</sup> ions/s-cm<sup>2</sup> and fluences up to 10<sup>8</sup> ions/cm<sup>2</sup> were used for the exposures. Run duration was approximately 2 minutes to achieve 10<sup>7</sup> fluence and approximately 20 minutes for the 10<sup>8</sup> fluence. Run conditions are summarized in [Table 4](#). No SEB was observed under any of the runs, indicating that the TPS50601A-SP is SEB/SEGR immune at T = Room Temp and LET up to 73.28 MeV-cm<sup>2</sup>/mg at 6 A. A typical  $P_{VIN} = V_{IN}$  (tied together) current vs time plot for run #6 is shown in [Figure 7](#).

Upper-bound SEB cross sections were calculated based on 0 events observed using a 95% confidence interval (see [Appendix B](#) for discussion of confidence limits):

$$\sigma_{SEB} \leq 7.36 \times 10^{-8} \text{ cm}^2/\text{device } LET_{EFF} = 73.2 \text{ MeV-cm}^2/\text{mg}, T = \text{Room Temp}, 95\% \text{ conf.}$$

**Table 4. Summary of TPS50601A-SP SEB Results**

RUN #	DEV #	Facility	Ion Type	Angle of Incidence (°)	$LET_{EFF}$ (MeV-cm <sup>2</sup> /mg)	FLUX (ions/s-cm <sup>2</sup> )	FLUENCE (ions/cm <sup>2</sup> )	VIN (V)	LOAD (A)	SEB ??
1	1	TAMU	Pr	0	66.42	1.05E+05	1.01E+07	7	6	No
2	1	TAMU	Pr	0	66.42	1.06E+05	2.93E+07	7	6	No
3	2	TAMU	Pr	0	66.42	1.13E+05	1.00E+07	7	6	No
4	2	TAMU	Pr	0	66.42	1.20E+05	1.00E+08	7	6	No
5	3	Berkeley	Xe	30	73.28	1.42E+05	5.01E+07	7	6	No
6	4	TAMU	Pr	28	74.82	1.33E+05	1.00E+08	5	3	No

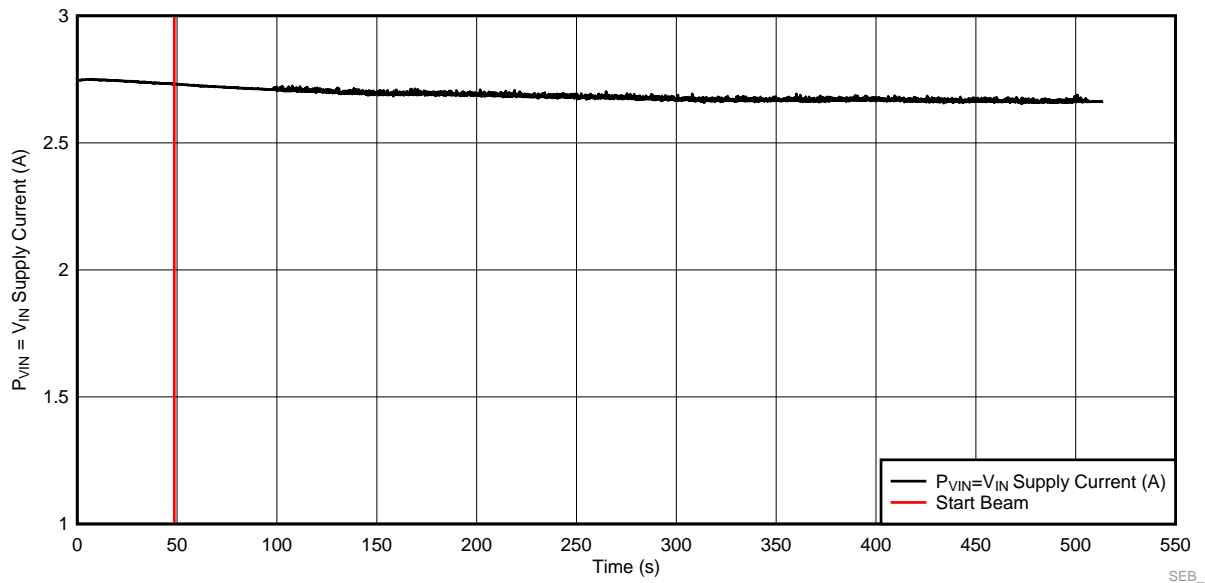


Figure 7. Current vs Time for SEB Run #6 at Room Temp, 73.28 MeV-cm<sup>2</sup>/mg, 6-A Load, and P<sub>VIN</sub> = V<sub>IN</sub> = 7 V

## 7.2 Single Event Latch-Up (SEL) Results

All SEL characterization was performed with forced hot air to maintain the die temperature at 125°C during the tests. A K-type thermocouple attached to the thermal pad vias with thermal paste was used to monitor the temperature. The thermocouple was calibrated using a thermal IR camera. The device was exposed to a Praseodymium (Pr) heavy-ion beam incident on the die surface at 0° and 28° for an effective LET of 66.42 and 74.82 MeV-cm<sup>2</sup>/mg respectively. A total fluence of 10<sup>7</sup> ions/cm<sup>2</sup> was used in all runs. Run duration to achieve this fluence was approximately 2 minutes. The SEL results are summarized in Table 5. No SEL event was observed under any of the test runs, at P<sub>VIN</sub> = V<sub>IN</sub> = 6.3 V and P<sub>VIN</sub> = V<sub>IN</sub> = 7 V (maximum recommended voltage), indicating that the TPS50601A-SP is SEL-immune at the full electrical specifications, T = 125°C, and LET<sub>EFF</sub> up to 74.82 MeV-cm<sup>2</sup>/mg.

Table 5. Summary of TPS50601A-SP SEL Results With T = 125°C

RUN #	DEV #	Die Temp (°C)	Ion Type	Angle of Incidence (°)	LET <sub>EFF</sub> (MeV-cm <sup>2</sup> /mg)	FLUX (ions/s-cm <sup>2</sup> )	FLUENCE (ions/cm <sup>2</sup> )	VIN (V)	VO (V)	LOAD (A)	SEL EVENTS <sup>(1)</sup>
7	5	125	Pr	28	74.82	1.03E+05	1.00E+07	7	2.5	6	0
8	5	125	Pr	28	74.82	1.02E+05	9.99E+06	6.3	2.5	6	0
9	5	123	Pr	28	74.82	9.85E+04	1.00E+07	6.3	2.5	6	0
10	5	125	Pr	28	74.82	1.03E+05	9.99E+06	6.3	2.5	6	0
11	5	123	Pr	28	74.82	1.01E+05	1.00E+07	6.3	2.5	6	0

<sup>(1)</sup> No SEL events were observed for any of the runs under the full range of load conditions.

Upper-bound SEL cross sections was calculated based on 0 events observed using a 95% confidence interval (see Appendix B for discussion of confidence limits):

$$\sigma_{\text{SEL}} \leq 3.69 \times 10^{-7} \text{ cm}^2/\text{device LET}_{\text{EFF}} = 74.82 \text{ MeV-cm}^2/\text{mg}, T = 45^\circ\text{C}, 95\% \text{ conf.}$$

## 8 Single-Event-Transient (SET) Results

In the case of the TPS50601A-SP, SETs were categorized as heavy-ion-induced events that create a fully recoverable transient on the output voltage ( $V_{OUT}$ ) or Power Good Flag ( $P_{GOOD}$ ). Such variations were monitored and captured using three digitizer modules monitoring  $V_{OUT}$ ,  $P_{GOOD}$ , and Soft Start (SS) continuously. A data record was captured any time the trigger conditions were achieved. All SET data was collected at room temperature, full load (6 A),  $P_{VIN} = V_{IN} = 5$  V, and  $V_{OUT} = 2.5$  V. Output filter (L-C) and compensations components used are shown in [Figure 3](#). The device was exposed to Argon ( $^{40}\text{Ar}$ ), Copper ( $^{63}\text{Cu}$ ), Silver ( $^{109}\text{Ag}$ ), and Xenon ( $^{136}\text{Xe}$ ) at angle of incidence of  $0^\circ$  at Berkeley 88-inch cyclotron (using the 10-MeV/amu line). Also Praseodymium ( $^{141}\text{Pr}$ ) ions were used at angles of  $0^\circ$  and  $28^\circ$  at the Texas A&M cyclotron (using the 15-MeV/amu line). Using these ions and angles, the  $LET_{EFF}$  is found to be between 10.11 to 75 MeV-cm<sup>2</sup>/mg, as discussed in [Section 5](#). Flux of  $10^5$  ions/s-cm<sup>2</sup> and fluences up to  $10^7$  ions/cm<sup>2</sup> were used for the exposures. Run duration to achieve  $10^7$  fluence was approximately 2 minutes. Run conditions are summarized in [Table 6](#).

Two NI-PXIe-5105 digitizer were used to capture any upsets on  $V_{OUT}$  and  $P_{GOOD}$ . Any deviation on  $V_{OUT}$  was captured using a window trigger with limits set around the nominal voltage ( $V_{OUT} = 2.5$  V). Limits as low as 3% around the nominal voltage were used during the characterization. On this scope card  $P_{VIN} = V_{IN}$ , EN,  $V_{SENSE}$ , and REFCAP were also monitored during a trigger. Deviations on  $P_{GOOD}$  were captured using an edge negative trigger set at half the  $V_{IN}$  voltage (2.5 V). On this scope card,  $V_{OUT}$  was also monitored. Scope card connections are shown on [Figure 6](#). **Not a Single  $P_{GOOD}$  upset was observed.**

Not a single upset exceeding the critical  $\pm 5\%$  variation (FPGA, CPU, and MCU regulations limits for most cases) on the output voltage was observed.

Transients inside  $\pm 5\%$  around the nominal voltage were observed and captured on the output voltage. All the signals were self-recoverable within a few milliseconds. For each upset, the maximum and minimum value was recorded and normalized with respect to the nominal value and shown on the histogram plots on [Figure 8](#) and [Figure 9](#), respectively. Transient recovery time for each upset was also recorded and shown in [Figure 10](#). Transient time was calculated as the time that output voltage crosses the trigger level and returns to the nominal voltage. All data was post-processed with a de-noising filter to remove all embedded noise from the capture cards. [Figure 11](#) shows the worse case positive deviation observed, [Figure 12](#) shows the worse case negative observed deviation, and [Figure 13](#) shows the worse case transient recovery time observed.

One Tektronix DPO 7104C was used to monitor the SS signal. Any deviation exceeding an edge negative trigger set at 0.5 V, triggered a capture. The value is selected based on internal functionality, since this is the voltage that will trigger a soft start (or restart cycle). On this scope,  $V_{OUT}$ , Phase, and  $P_{GOOD}$  were also monitored. Not a single restart cycle (or trigger) was captured during the characterization of the TPS50601A-SP. Such behavior is considered a SEFI, making the TPS50601A-SP SEFI-free.

**Table 6. Summary of TPS50601A-SP SET Results**

RUN #	DEV #	Die Temp (°C)	Ion Type	Angle of Incidence (°)	LET <sub>EFF</sub> (MeV-cm <sup>2</sup> /mg)	FLUX (ions/s-cm <sup>2</sup> )	FLUENCE (ions/cm <sup>2</sup> )	VIN (V)	VO (V)	LOAD (A)	SET >  ±5%
12	6	45	Ar	0	10.11	9.54E+04	1.00E+07	5	2.5	6	0
13	6	45	Ar	0	10.11	9.54E+04	1.00E+07	5	2.5	6	0
14	6	45	Ar	0	10.11	9.54E+04	1.00E+07	5	2.5	6	0
15	6	45	Ar	0	10.11	9.54E+04	1.00E+07	5	2.5	6	0
16	6	45	Cu	0	21.75	7.48E+04	1.00E+07	5	2.5	6	0
17	6	45	Cu	0	21.75	7.48E+04	1.00E+07	5	2.5	6	0
18	6	45	Ag	0	50.4	4.30E+04	1.00E+07	5	2.5	6	0
19	6	45	Ag	0	50.4	4.30E+04	1.00E+07	5	2.5	6	0
20	6	45	Xe	0	62.33	6.68E+04	4.19E+06	5	2.5	6	0
21	6	45	Xe	0	62.33	6.68E+04	1.00E+07	5	2.5	6	0
22	6	45	Xe	0	62.33	1.00E+05	4.19E+06	5	2.5	6	0
24	7	45	Pr	0	66.42	9.99E+04	1.01E+07	5	2.5	6	0
25	7	45	Pr	0	66.42	9.90E+04	1.00E+07	5	2.5	6	0
23	7	45	Pr	28	75	9.39E+04	1.00E+07	5	2.5	6	0

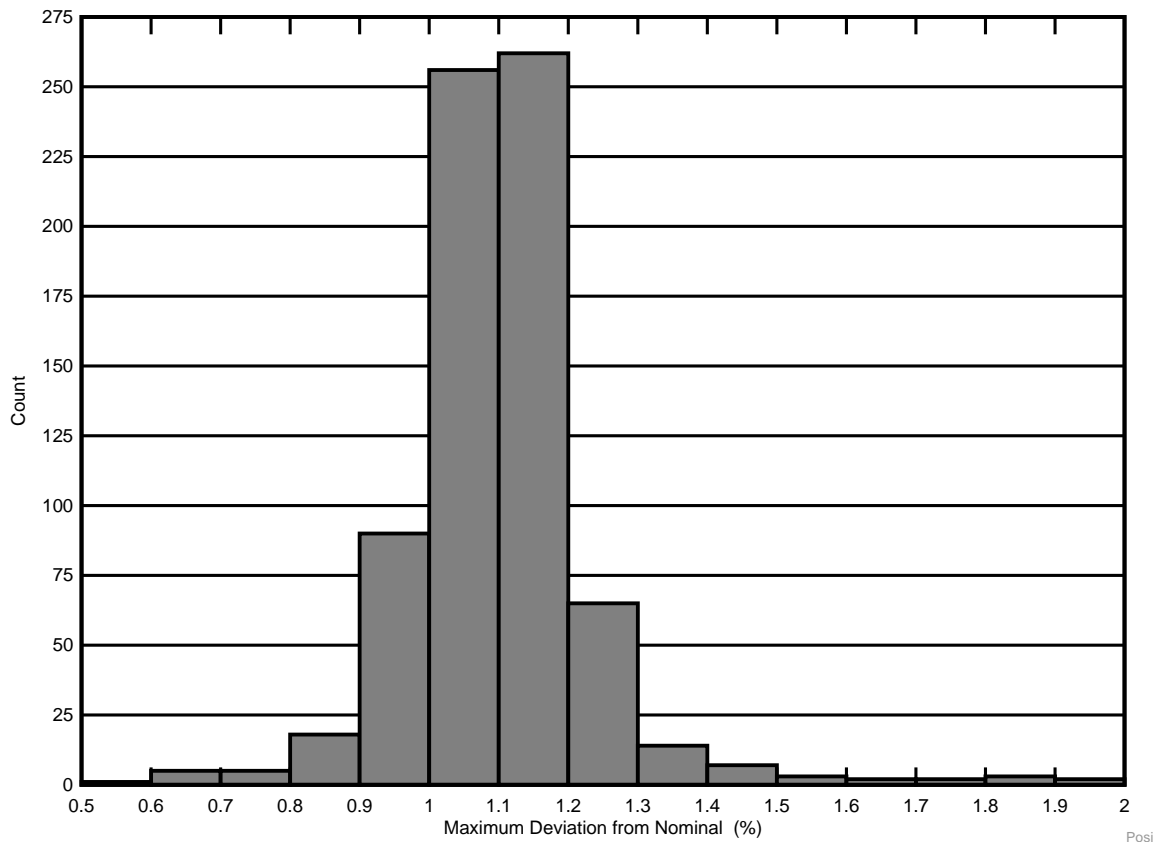


**Figure 8. Histogram of the Normalized Maximum Value for All Captured SETs Across All LET<sub>EFF</sub>**

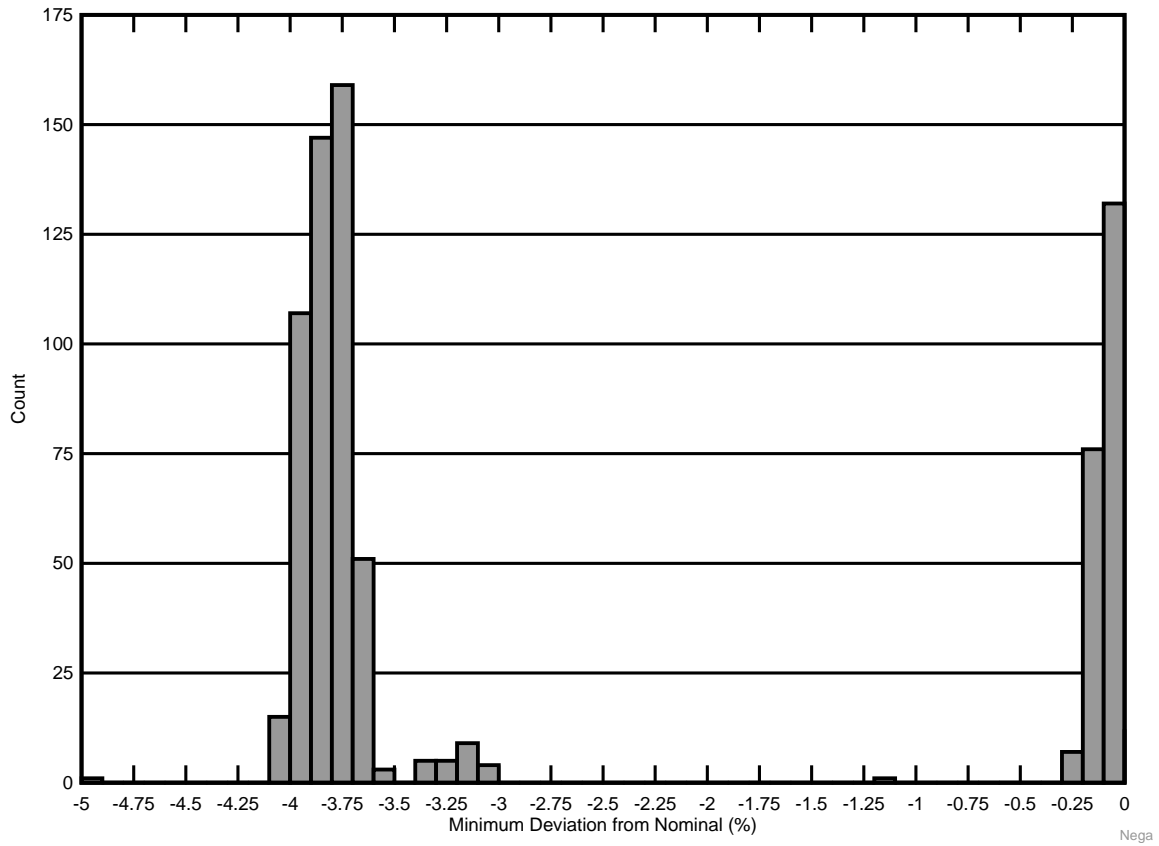


**Figure 9. Histogram of the Normalized Minimum Value for All Captured SETs Across All LET<sub>EFF</sub>**

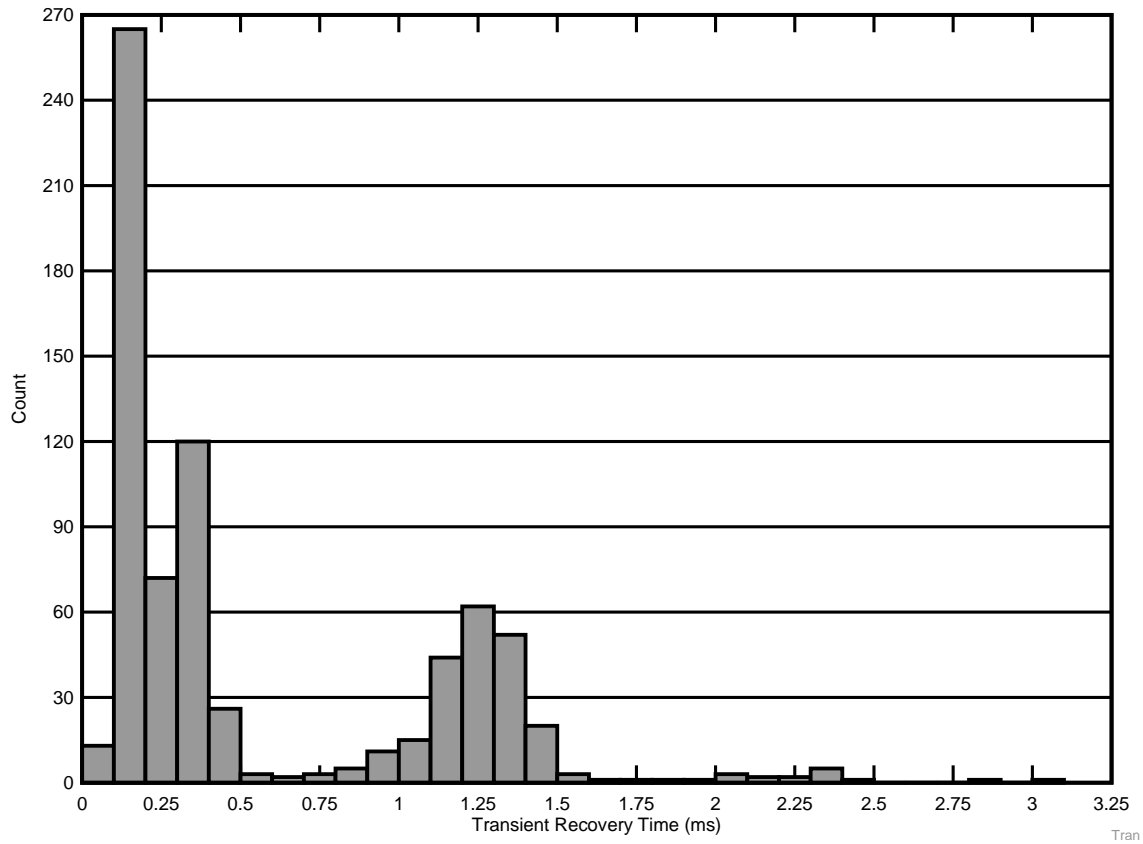


Figure 10. Histogram of the Transient Recovery Time for All Captured SETs Across All LET<sub>EFF</sub>

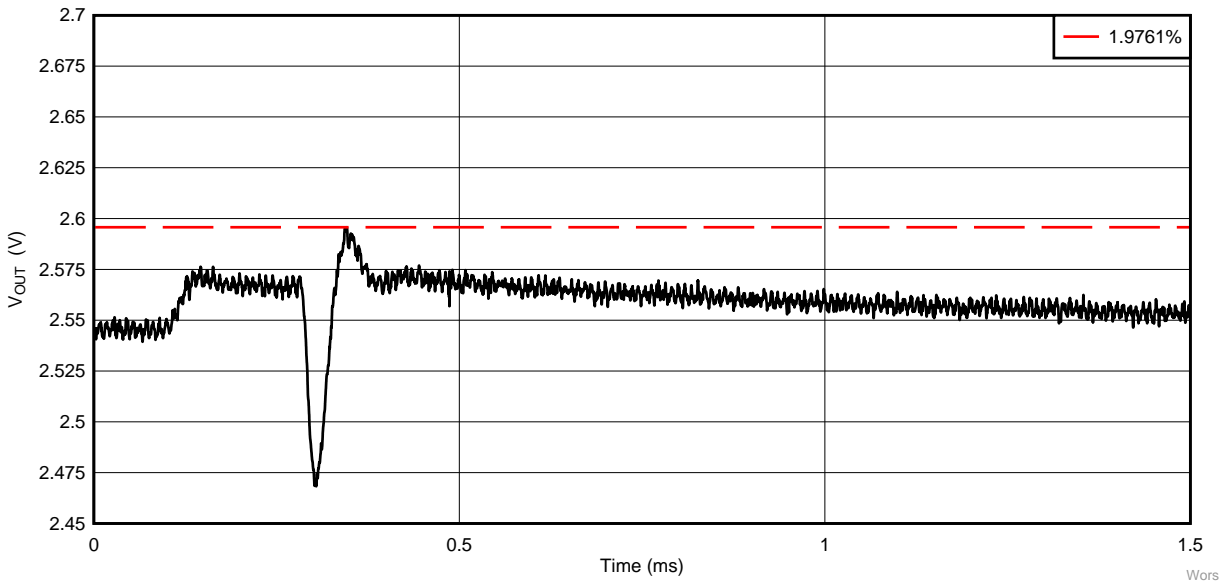
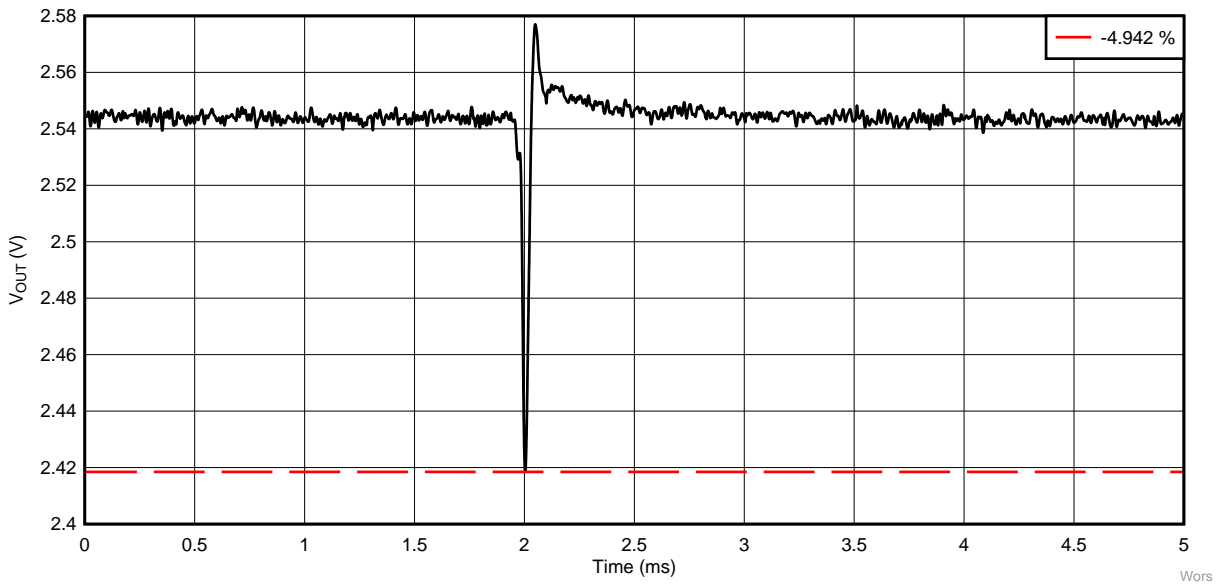
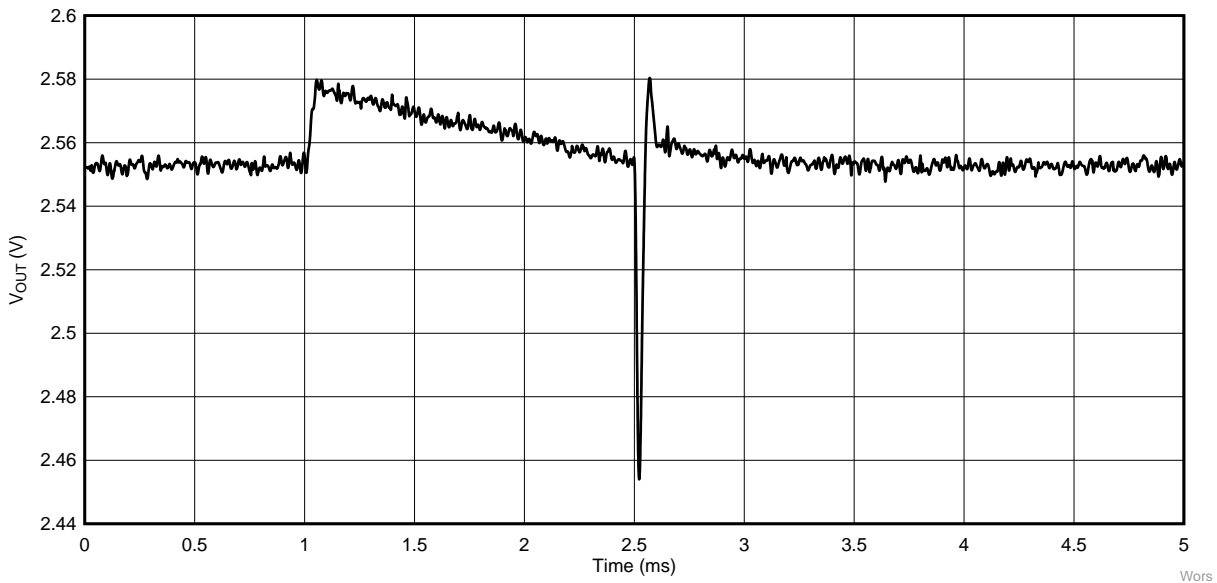


Figure 11. Time Domain Plot for the Worst Case Positive Deviation Observed



**Figure 12. Time Domain Plot for the Worst Case Negative Deviation Observed**



**Figure 13. Time Domain Plot for the Worst Case Transient Recovery Time Observed**

Upper-bound SET cross sections were calculated based on 0 events (for  $\pm 5\%$  deviations) observed using a 95% confidence interval (see [Appendix B](#) for discussion of confidence limits):

$$\sigma_{V_{OUT-SET}} \leq 3.69 \times 10^{-7} \text{ cm}^2/\text{device LET}_{EFF} = 74.82 \text{ MeV-cm}^2/\text{mg}, T = \text{Room Temp}, 95\% \text{ conf.}, \text{ and } \geq 5\% \text{ from nominal}$$

$$\sigma_{P_{GOOD-SET}} \leq 3.69 \times 10^{-7} \text{ cm}^2/\text{device LET}_{EFF} = 74.82 \text{ MeV-cm}^2/\text{mg}, T = \text{Room Temp}, \text{ and } 95\% \text{ conf.}$$

## 9 Event Rate Calculations

Events rates were calculated for LEO (ISS) and GEO environments by combining CREME96 orbital integral flux estimations. With zero upsets observed for SEL, SEB,  $V_{OUT} - SET > \pm 5\%$  from nominal output voltage, and  $P_{GOOD} - SET$ , the error rate was calculated using the upper bound cross section calculated as discussed in [Appendix B](#) and the integral flux at  $\sim LET_{EFF} = 74.82 \text{ MeV-cm}^2/\text{mg}$  for LEO (ISS) and GEO as discussed in [Appendix C](#). A minimum shielding of 100 mils (2.54 mm) of aluminum and "worst week" solar activity was assumed. "Worst Week" is similar to 99% upper bound for the environment. [Table 7](#) to [Table 9](#) shows the error rates for these two environments for SEB, SEL, and  $SET > \pm 5\%$  from nominal.

**Table 7. SEB Event Rate Calculations for Worst-Week LEO and GEO Orbits**

Orbit Type	Onset $LET_{EFF}$ (MeV-cm <sup>2</sup> /mg)	CREME96 Integral FLUX (/day-cm <sup>2</sup> )	$\sigma_{SAT}$ (cm <sup>2</sup> )	Event Rate (/day)	Event Rate (FIT)	MTBE (Years)
LEO (ISS)	73.2	7.40E-05	7.36303E-08	5.45E-12	0.000227	5.03E+08
GEO		2.10E-04		1.54E-11	0.000643	1.78E+08

**Table 8. SEL Event Rate Calculations for Worst-Week LEO and GEO Orbits**

Orbit Type	Onset $LET_{EFF}$ (MeV-cm <sup>2</sup> /mg)	CREME96 Integral FLUX (/day-cm <sup>2</sup> )	$\sigma_{SAT}$ (cm <sup>2</sup> )	Event Rate (/day)	Event Rate (FIT)	MTBE (Years)
LEO (ISS)	74.82	6.25E-05	3.68888E-07	2.31E-11	0.000961	1.19E+08
GEO		1.77E-04		6.51E-11	0.002713	4.21E+07

**Table 9.  $V_{OUT} - SET > \pm 5\%$  From Nominal Voltage and  $P_{GOOD}$  Event Rate Calculations for Worst-Week LEO and GEO Orbits**

Orbit Type	Onset $LET_{EFF}$ (MeV-cm <sup>2</sup> /mg)	CREME96 Integral FLUX (/day-cm <sup>2</sup> )	$\sigma_{SAT}$ (cm <sup>2</sup> )	Event Rate (/day)	Event Rate (FIT)	MTBE (Years)
LEO (ISS)	74.82	6.25E-05	3.68888E-07	2.31E-11	0.000961	1.19E+08
GEO		1.77E-04		6.51E-11	0.002713	4.21E+07

## 10 Summary

The purpose of this report is to summarize all data collected on the TPS50601A-SP. The data shows the TPS50601A-SP is SEB-, SEGR-, and SEL-free across the full electrical specifications and up to  $LET_{EFF} = 74.82 \text{ MeV-cm}^2/\text{mg}$ . It also shows the TPS50601A-SP is  $V_{OUT}$  SET free for upsets greater than  $\pm 5\%$  from the nominal voltage and  $P_{GOOD}$  at the conditions tested. Histograms for the magnitude deviation and transient time recovery for upsets inside the  $\pm 5\%$  from nominal are presented. Worst case time domain voltage excursion plots on  $V_{OUT}$  are also presented.

## ***Total Ionizing Dose From SEE Experiments***

---

---

---

The production TPS60501A-SP POL is rated to a total ionizing dose (TID) of 100 krad(Si). In the course of the SEE testing, the heavy-ion exposures delivered  $\approx 10$  krad(Si) per  $10^7$  ions/cm<sup>2</sup> run. The cumulative TID exposure for each device respectively, over all runs they underwent, was determined to be below the 100 krad(Si). All qualified production devices used in the studies described in this report stayed within specification and were fully-functional after the heavy-ion SEE testing was completed.

## Confidence Interval Calculations

---



---

For conventional products where hundreds of failures are seen during a single exposure, one can determine the average failure rate of parts being tested in a heavy-ion beam as a function of fluence with high degree of certainty and reasonably tight standard deviation, and thus have a good deal of confidence that the calculated cross section is accurate.

With radiation hardened parts however, determining the cross section becomes more difficult since often few, or even, no failures are observed during an entire exposure. Determining the cross section using an average failure rate with standard deviation is no longer a viable option, and the common practice of assuming a single error occurred at the conclusion of a null-result can end up in a greatly underestimated cross section.

In cases where observed failures are rare or non-existent, the use of confidence intervals and the chi-squared distribution is indicated. The Chi-Squared distribution is particularly well-suited for the determination of a reliability level when the failures occur at a constant rate. In the case of SEE testing, where the ion events are random in time and position within the irradiation area, one expects a failure rate that is independent of time (presuming that parametric shifts induced by the total ionizing dose do not affect the failure rate), and thus the use of chi-squared statistical techniques is valid (since events are rare an exponential or Poisson distribution is usually used).

In a typical SEE experiment, the device-under-test (DUT) is exposed to a known, fixed fluence (ions/cm<sup>2</sup>) while the DUT is monitored for failures. This is analogous to fixed-time reliability testing and, more specifically, time-terminated testing, where the reliability test is terminated after a fixed amount of time whether or not a failure has occurred (in the case of SEE tests fluence is substituted for time and hence it is a fixed fluence test) [14]. Calculating a confidence interval specifically provides a range of values which is likely to contain the parameter of interest (the actual number of failures/fluence). Confidence intervals are constructed at a specific confidence level. For example, a 95% confidence level implies that if a given number of units were sampled numerous times and a confidence interval estimated for each test, the resulting set of confidence intervals would bracket the true population parameter in about 95% of the cases.

In order to estimate the cross section from a null-result (no fails observed for a given fluence) with a confidence interval, we start with the standard reliability determination of lower-bound (minimum) mean-time-to-failure for fixed-time testing (an exponential distribution is assumed):

$$MTTF = \frac{2nT}{\chi^2_{2(d+1); 100\left(1-\frac{\alpha}{2}\right)}} \quad (1)$$

Where *MTTF* is the minimum (lower-bound) mean-time-to-failure, *n* is the number of units tested (presuming each unit is tested under identical conditions) and *T*, is the test time, and  $\chi^2$  is the chi-square distribution evaluated at  $100(1 - \alpha / 2)$  confidence level and where *d* is the degrees-of-freedom (the number of failures observed). With slight modification for our purposes we invert the inequality and substitute *F* (fluence) in the place of *T*:

$$MFTF = \frac{2nF}{\chi^2_{2(d+1); 100\left(1-\frac{\alpha}{2}\right)}} \quad (2)$$

Where now *MFTF* is mean-fluence-to-failure and *F* is the test fluence, and as before,  $\chi^2$  is the chi-square distribution evaluated at  $100(1 - \alpha / 2)$  confidence and where *d* is the degrees-of-freedom (the number of failures observed). The inverse relation between MTTF and failure rate is mirrored with the MFTF. Thus the upper-bound cross section is obtained by inverting the MFTF:

$$\sigma = \frac{\chi^2_{2(d+1); 100\left(1-\frac{\alpha}{2}\right)}}{2nF} \quad (3)$$

Let's assume that all tests are terminated at a total fluence of  $10^6$  ions/cm<sup>2</sup>. Let's also assume that we have a number of devices with very different performances that are tested under identical conditions. Assume a 95% confidence level ( $\sigma = 0.05$ ). Note that as  $d$  increases from 0 events to 100 events the actual confidence interval becomes smaller, indicating that the range of values of the true value of the population parameter (in this case the cross section) is approaching the mean value + 1 standard deviation. This makes sense when one considers that as more events are observed the statistics are improved such that uncertainty in the actual device performance is reduced.

**Table 10. Experimental Example Calculation of Mean-Fluence-to-Failure (MFTF) and  $\sigma$  Using a 95% Confidence Interval<sup>(1)</sup>**

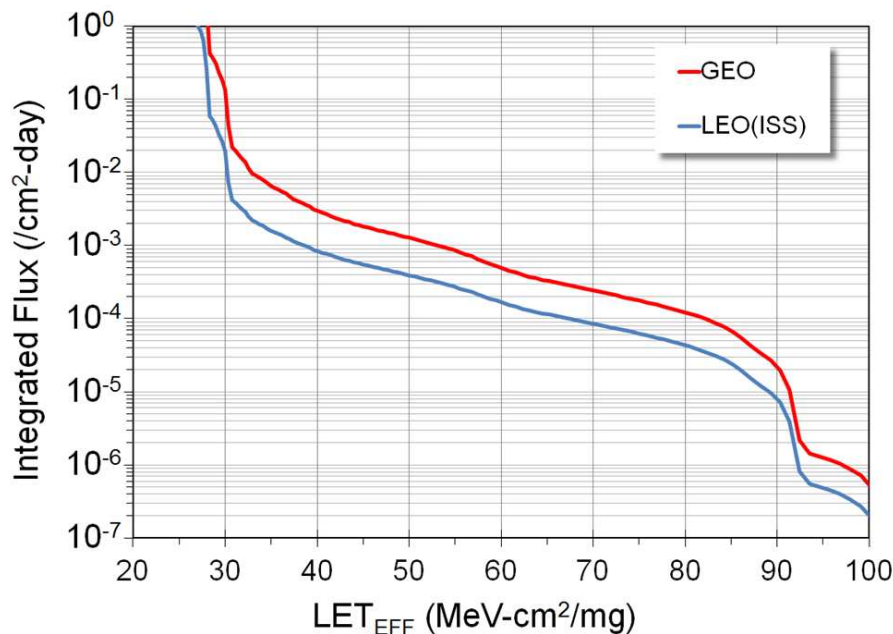
Degrees-of-Freedom (d)	2(d + 1)	$\chi^2$ @ 95%	Calculated Cross Section (cm <sup>2</sup> )		
			Upper-Bound @ 95% Confidence	Mean	Average + Standard Deviation
0	2	7.38	3.69E-06	0.00E+00	0.00E+00
1	4	11.14	5.57E-06	1.00E-06	2.00E-06
2	6	14.45	7.22E-06	2.00E-06	3.41E-06
3	8	17.53	8.77E-06	3.00E-06	4.73E-06
4	10	20.48	1.02E-05	4.00E-06	6.00E-06
5	12	23.34	1.17E-05	5.00E-06	7.24E-06
10	22	36.78	1.84E-05	1.00E-05	1.32E-05
50	102	131.84	6.59E-05	5.00E-05	5.71E-05
100	202	243.25	1.22E-04	1.00E-04	1.10E-04

<sup>(1)</sup> Using a 95% confidence for several different observed results (d = 0, 1, 2...100 observed events during fixed-fluence tests) assuming  $10^6$  ion/cm<sup>2</sup> for each test.

## Orbital Environment Estimations

In order to calculate on-orbit SEE event rates one needs both the device SEE cross section and the flux of particles encountered in a particular orbit. Device SEE cross sections are usually determined experimentally while flux of particles in orbit is calculated using various codes. For the purpose of generating some event rates, a Low-Earth Orbit (LEO) and a Geostationary-Earth Orbit (GEO) were calculated using CREME96. CREME96 code, short for Cosmic Ray Effects on Micro-Electronics is a suite of programs [15][16] that enable estimation of the radiation environment in near-Earth orbits. CREME96 is one several tools available in the aerospace industry to provide accurate space environment calculations. Over the years since its introduction, the CREME models have been compared with on-orbit data and demonstrated their accuracy. In particular, CREME96 incorporates realistic “worst-case” solar particle event models, where fluxes can increase by several orders-of-magnitude over short periods of time.

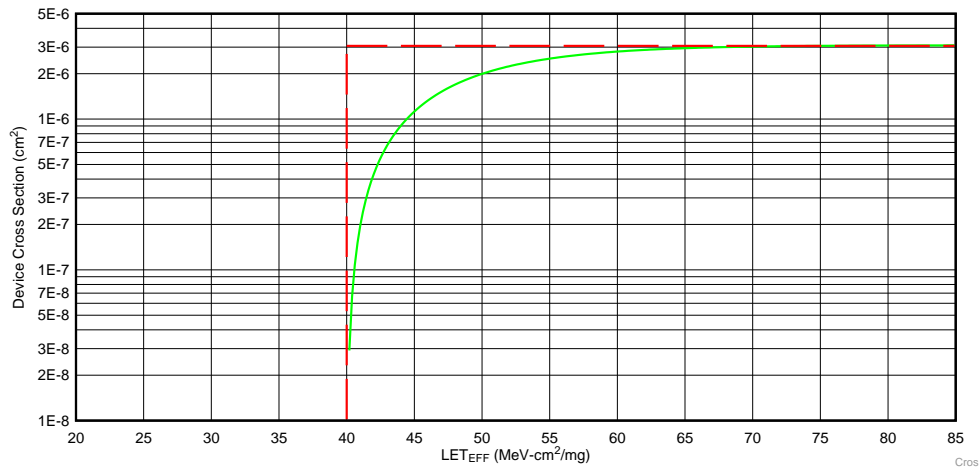
For the purposes of generating conservative event rates, the worst-week model (based on the biggest solar event lasting a week in the last 45 years) was selected, which has been equated to a 99%-confidence level worst-case event [17][18]. The integrated flux includes protons to heavy ions from solar and galactic sources. A minimal shielding configuration is assumed at 100 mils (2.54 mm) of aluminum. Two orbital environments were estimated, that of the International Space Station (ISS), which is LEO, and the GEO environment. Figure 14 shows the integrated flux (from high LET to low) for these two environments.



- (1) LEO(ISS) (blue) and a GEO (red) environment as calculated by CREME96, assuming worst-week and 100 mils (2.54 mm) of aluminum shielding.

**Figure 14. Integral Particle Flux vs LET<sub>EFF</sub>**

Using this data, we can extract integral particle fluxes for any arbitrary LET of interest. To simplify the calculation of event rates we assume that all cross section curves are square – meaning that below the onset LET the cross section is identically zero while above the onset LET the cross section is uniformly equal to the saturation cross section. Figure 15 illustrates the approximation, with the green curve being the actual Weibull fit to the data with the “square” approximation shown as the red-dashed line. This allows us to calculate event rates with a single multiplication, the event rate becoming simply the product of the integral flux at the onset LET, and the saturation cross section. Obviously this leads to an overestimation of the event rate since the area under the square approximation is larger than the actual cross section curve – but for the purposes of calculating upper-bound event rate estimates, this modification avoids the need to do the integral over the flux and cross section curves.



(1) Weibull Fit (green) is “simplified” with the use of a square approximation (red dashed line).

**Figure 15. Device Cross Section vs LET<sub>EFF</sub>**

To demonstrate how the event rates in this report were calculated, assume that we wish to calculate an event rate for a GEO orbit for the device whose cross section is shown in Figure 15. Using the red curve in Figure 14 and the onset LET value obtained from Figure 15 (~40 MeV-cm<sup>2</sup>/mg) we find the GEO integral flux to be ~2.97 × 10<sup>-3</sup> ions/cm<sup>2</sup>-day. The event rate is the product of the integral flux and the saturation cross section in Figure 15 (~3.09 × 10<sup>-6</sup> cm<sup>2</sup>):

$$GEO \text{ Event Rate} = \left( 2.97 \times 10^{-3} \frac{\text{ions}}{\text{cm}^2 \times \text{day}} \right) \times (3.09 \times 10^{-6} \text{ cm}^2) = 9.17 \times 10^{-9} \frac{\text{events}}{\text{day}} \tag{4}$$

$$GEO \text{ Event Rate} = 3.82 \times 10^{-10} \frac{\text{events}}{\text{hr}} = 0.382 \text{ FIT} \tag{5}$$

$$MTBF = 298901 \text{ Years !} \tag{6}$$

---

---

## References

---

---

- (1) G. H. Johnson, R. D. Schrimpf, K. F. Galloway, and R. Koga, "Temperature dependence of single-event burnout in n-channel power MOSFETs [for space application]," *IEEE Trans. Nucl. Sci.*, Vol. 39(6), Dec. 1992, pp. 1605–1612.
- (2) D. K. Nichols, J. R. Coss, and K. P. McCarty, "Single event gate rupture in commercial power MOSFETs," *Radiation and its Effects on Components and Systems*, Sept. 1993, pp. 462–467.
- (3) M. Shoga and D. Binder, "Theory of Single Event Latchup in Complementary Metal-Oxide Semiconductor ICs," *IEEE Trans. Nucl. Sci.*, Vol. 33(6), Dec. 1986, pp. 1714–1717.
- (4) G. Bruguier and J.M. Palau, "Single particle-induced latchup," *IEEE Trans. Nucl. Sci.*, Vol. 43(2), Mar. 1996, pp. 522–532.
- (5) J. M. Hutson, R. D. Schrimpf, and L. W. Massengill, "The effects of scaling and well and substrate contact placement on single event latchup in bulk CMOS technology," in *Proc. RADECS*, Sept. 2005, pp. PC24-1–PC24-5.
- (6) N. A. Dodds, J. M. Hutson, J. A. Pellish, et al., "Selection of Well Contact Densities for Latchup-Immune Minimal-Area ICs," *IEEE Trans. Nucl. Sci.*, Vol. 57(6), Dec. 2010, pp. 3575–3581.
- (7) D. B. Estreich and A. Ochoa, Jr., and R. W. Dutton, "An Analysis of Latch-Up Prevention in CMOS IC's Using an Epitaxial-Buried Layer Process," *Proceed. IEEE Elec. Dev. Meeting*, 24, Dec. 1978, pp. 230–234.
- (8) R. Krithivasan, et al., "Application of RHBD techniques to SEU hardening of Third-Generation SiGe HBT Logic Circuits," *IEEE Trans. Nucl. Sci.*, Vol. 53(6), Dec. 2006, pp. 3400–3407.
- (9) P. C. Adell, R. D. Schrimpf, B. K. Choi, W. T. Holman, J. P. Attwood, C. R. Cirba, and K. F. Galloway, "Total-Dose and Single-Event Effects in Switching DC/DC Power Converters," *IEEE Trans. Nucl. Sci.* Vol. 49(6), Dec. 2002, pp. 3217–3221.
- (10) R. L. Pease, "Modeling Single Event Transients in Bipolar Linear Circuits," *IEEE Trans. Nucl. Sci.*, Vol. 55(4), Aug. 2008, pp. 1879–1890.
- (11) R. Lveugle and A. Ammari, "Early SEU Fault Injection in Digital, Analog and Mixed Signal Circuits: a Global Flow," *Proc. of Design, Automation and Test in Europe Conf.*, 2004, pp. 1530–1591.
- (12) TAMU Radiation Effects Facility website. <http://cyclotron.tamu.edu/ref/>
- (13) "The Stopping and Range of Ions in Matter" (SRIM) software simulation tools website. <http://www.srim.org/index.htm#SRIMMENU>
- (14) D. Kececioglu, "Reliability and Life Testing Handbook", Vol. 1, PTR Prentice Hall, New Jersey, 1993, pp. 186–193.
- (15) <https://creme.isde.vanderbilt.edu/CREME-MC>
- (16) A. J. Tylka, et al., "CREME96: A Revision of the Cosmic Ray Effects on Micro-Electronics Code", *IEEE Trans. Nucl. Sci.*, Vol. 44(6), 1997, pp. 2150–2160.
- (17) A. J. Tylka, W. F. Dietrich, and P. R. Boberg, "Probability distributions of high-energy solar-heavy-ion fluxes from IMP-8: 1973–1996", *IEEE Trans. Nucl. Sci.*, Vol. 44(6), Dec. 1997, pp. 2140–2149.
- (18) A. J. Tylka, J. H. Adams, P. R. Boberg, et al., "CREME96: A Revision of the Cosmic Ray Effects on Micro-Electronics Code", *IEEE Trans. Nucl. Sci.*, Vol. 44(6), Dec. 1997, pp. 2150–2160.

## IMPORTANT NOTICE AND DISCLAIMER

TI PROVIDES TECHNICAL AND RELIABILITY DATA (INCLUDING DATA SHEETS), DESIGN RESOURCES (INCLUDING REFERENCE DESIGNS), APPLICATION OR OTHER DESIGN ADVICE, WEB TOOLS, SAFETY INFORMATION, AND OTHER RESOURCES "AS IS" AND WITH ALL FAULTS, AND DISCLAIMS ALL WARRANTIES, EXPRESS AND IMPLIED, INCLUDING WITHOUT LIMITATION ANY IMPLIED WARRANTIES OF MERCHANTABILITY, FITNESS FOR A PARTICULAR PURPOSE OR NON-INFRINGEMENT OF THIRD PARTY INTELLECTUAL PROPERTY RIGHTS.

These resources are intended for skilled developers designing with TI products. You are solely responsible for (1) selecting the appropriate TI products for your application, (2) designing, validating and testing your application, and (3) ensuring your application meets applicable standards, and any other safety, security, regulatory or other requirements.

These resources are subject to change without notice. TI grants you permission to use these resources only for development of an application that uses the TI products described in the resource. Other reproduction and display of these resources is prohibited. No license is granted to any other TI intellectual property right or to any third party intellectual property right. TI disclaims responsibility for, and you will fully indemnify TI and its representatives against, any claims, damages, costs, losses, and liabilities arising out of your use of these resources.

TI's products are provided subject to [TI's Terms of Sale](#) or other applicable terms available either on [ti.com](#) or provided in conjunction with such TI products. TI's provision of these resources does not expand or otherwise alter TI's applicable warranties or warranty disclaimers for TI products.

TI objects to and rejects any additional or different terms you may have proposed.

Mailing Address: Texas Instruments, Post Office Box 655303, Dallas, Texas 75265  
Copyright © 2022, Texas Instruments Incorporated